JOURNAL OF MATERIALS SCIENCE 21 (1986) 1981–1989

Deformation and fracture of yttria-stabilized zirconia single crystals

JAMES LANKFORD
Southwest Research Institute, San Antonio, Texas 78284, USA

Deformation and failure mechanisms are characterized for fully and partially yttria-stabilized single crystals tested in compression from 23 to 1150° C. It is found that both types of material exhibit extensive plastic flow over most of this temperature range, producing rapid decreases in strength with increasing temperature. Tetragonal to monoclinic transformation-induced plasticity is not observed; rather, plastic flow is related solely to dislocation activity. Evidence is found for apparent cubic to rhombohedral transformation during polishing, and reverse rhombohedral to cubic transformation during imposed compressive stress.

1. Introduction

Considerable interest has focused upon partially stabilized zirconia single crystals [1–3], which appear to possess a number of desirable technological properties. For example, these materials maintain their flexural strength to temperatures as high as 1500° C, their fracture toughness at elevated temperature increases with temperature, and they lack grain boundaries and grain-boundary phases which tend to promote intergranular failure at elevated temperature. Questions persist, however, regarding the role of stress-induced transformations in the strengthening and toughening of these ceramics, as opposed to polycrystalline MgO– and CaO–partially stabilized zirconias (PSZs), in which transformation-induced plasticity clearly is very important. Similarly, the relevant deformation and damage processes are not well understood. Finally, most of the work to date has involved a nominally tensile stress state, while certain technological applications, such as high-temperature bearings, will involve compressive or multiaxial loading. The present study seeks to address some of these issues.

Certain experimental results by other researchers provide an important background in this regard, particularly the papers by Ingel *et al.* [1, 2], based on the dissertation by Ingel [4], dealing with the mechanical properties of zirconia crystals stabilized with from 3 to 20 wt % Y_2O_3. Over most of the temperature range 23 to 1500° C, the strengths and fracture toughnesses of partially stabilized variants, i.e. ones with significant amounts of tetragonal phase (< 20 wt % Y_2O_3), considerably exceeded those for fully stabilized (cubic, $\gtrsim$ 20 wt % Y_2O_3) crystals. It was found further [2, 4] that partially-stabilized (6 wt % Y) bend specimens evidenced very little plasticity, even for temperatures as high as 1500° C. Cubic crystals, on the other hand, underwent a brittle ductile transition at around 1000 to 1200° C; at 1500° C, fracture could be either brittle or ductile, with from zero to 7.8% permanent strain, depending upon crystallographic orientation.

The fracture toughness of both partially and fully stabilized crystals decreased with increasing temperature up to ~ 1000° C, above which (roughly the maximum temperature for the tetragonal to monoclinic transformation) K_{Ic} was found to increase with temperature. The former effect was ascribed to reduction in toughening contributed by the tetragonal to monoclinic phase transformation, which was assumed to be operating. The high-temperature toughening was considered to be caused by crack–precipitate interactions, as reflected in the rough fracture surfaces of the PSZ specimens, and the smooth fractography of the fully stabilized ones. Michel *et al.* [3] likewise found predominantly tetragonal 5.4 wt % Y–ZrO_2 crystals tested at 23° C to be about three times tougher than the cubic-phase (16.2 wt % Y) material; however, Raman spectroscopy showed conclusively that the fracture surfaces of the specimens contained no monoclinic phase. Thus, the tetragonal to monoclinic transformation could not be responsible for the PSZ toughness. Instead, the greater toughness of the tetragonal phase crystals was attributed to a rough fracture mode (faceted on {0 0 1}), as against smooth cleavage on {1 1 1} for the cubic phase.

Interesting work related to these experiments was performed by Coyle, and described in his recent dissertation [5]. By also utilizing Raman spectroscopy, Coyle determined that the fracture surfaces of 6 wt % Y–PSZ specimens which failed in compression and in bending evidenced monoclinic transformed layers 50 and 15 μm thick, respectively. On the other hand, 5 wt % Y–PSZ which failed in bending had no monoclinic material on its fracture surface. These experiments demonstrate the sensitivity of the transformation process to stabilizer chemistry and precipitate microstructure.

Slip systems in yttria–cubic stabilized zirconia (Y–CSZ) and MgO-stabilized PSZ (Mg–PSZ) were studied by Hannink and Swain [6]. From hardness anisotropy, it was inferred that for both Y–CSZ and Mg–PSZ crystals, the active slip system between 23 and 600° C is either {0 0 1}⟨0 1 1⟩ or {1 1 1}⟨1 1 0⟩. Based on an earlier study of CaF_2 [7], and a TEM

0022–2461/86 $03.00 + .12

TABLE I Material properties

Material	Flexural strength (MPa)	Hardness (GPa)	Fracture toughness ($MPa\,m^{1/2}$)
20Y–CSZ (single crystal	196	15.3	1.9
5Y–PSZ (single crystal)	1384	13.6	6.9
Mg–PSZ (polycrystal)	600	10.2	8 to 15

study [8] of Ca–CSZ crystals deformed at 1350° C, it was assumed that the current system was $\{0\,0\,1\}\langle 0\,1\,1\rangle$. However, it was observed that Arrhenius plots of hardness against reciprocal temperature showed a distinct break at around 400° C, which normally indicates a change in thermally activated mechanism. As noted by the authors [6], this might be taken to suggest activity on another slip system.

Recent work by two independent groups in Japan [9, 10] has revealed a possible additional, complicating factor. Based on X-ray diffraction, it was determined that the cubic phase, for both Y–PSZ and, to a lesser extent, Y–CSZ, can apparently transform to a rhombohedral structure. This transformation occurs both by grinding/polishing [9], i.e. in thin surface layers, and also in the bulk [10], for certain compositions and, probably, certain heat treatments. It appears that the rhombohedral phase is quite unstable, and that the cubic → rhombohedral transformation is stress-assisted and reversible [10].

In order to explore the interrelationships between these factors, an experimental programme was performed involving compressive deformation of both fully and partially stabilized $Y–ZrO_2$ crystals. Since compressive microfracture is a relatively stable process, it is possible to generate damage under high stresses within the bulk of a specimen without failing it. This facilitates subsequent damage characterization, which is otherwise quite difficult to accomplish for the extremely localized high-stress regions attending crack tips, or their flanks, in tensile specimens.

2. Experimental procedure

Materials for specimens were provided by R. W. Rice of NRL, the crystals deriving from the same as-received batches* used in the work of Ingel [4]. Two compositions were studied, namely, 20 wt % Y_2O_3–ZrO_2 (20Y–CSZ), and 5 wt % Y_2O_3–ZrO_2 (5Y–PSZ); both were fully characterized by Ingel [4]. Briefly, however, the former were fully stabilized, and therefore had a cubic microstructure, while the latter consisted of a "tweed" microstructure, composed of ~ 50 vol % of tetragonal precipitates within a cubic matrix. The precipitates are coherent or semicoherent with the cubic matrix, and form distorted ellipsoids ranging in length from ~ 400 to ~ 1400 nm, and in width from ~ 80 to ~ 280 nm [4]. Ambient material condition properties of both compositions are given in Table I, together, for comparison, with corresponding properties for polycrystalline Mg–PSZ† tested earlier in compression [11].

Compression specimens in the form of right circular cylinders, ~ 9 mm long × 4.5 mm diameter, were machined from the crystals. The axis of each specimen was oriented near the centre of the standard cubic stereographic triangle, and provided approximately equal Schmid factors of approximately 0.45 for $\{0\,0\,1\}\langle 0\,1\,1\rangle$ and $\{1\,1\,1\}\langle 1\,1\,0\rangle$ slip. The ends of both the specimens and their alumina loading platens were precision-ground and lapped parallel to within 2 μm.

Compression tests were performed in air at a strain rate of $7 \times 10^{-5}\,sec^{-1}$, over a temperature range of 23 to 1150° C. In order to establish the threshold stress level for microfracture, an acoustic emission system was employed, as described in conjunction with a recent study of polycrystalline Mg–PSZ [11].

To facilitate damage characterization, extremely smooth (0.05 μm diamond) flats were polished on to certain specimens, which were subsequently loaded past yield and then unloaded. The flats were then examined using Nomarski microscopy and scanning electron microscopy (SEM) of palladium-coated flats, and transmission electron microscopy (TEM) of two-stage carbon surface replicas. Finally, some of these specimens were sectioned normal to their axes into thin wafers, which were ion-milled and examined as thin foils in the TEM.

3. Results

In the following section, the deformation and fracture of single-crystal 20Y–CSZ and 5Y–PSZ are compared with one another, and with polycrystalline Mg–PSZ [11]. Relevant damage mechanisms are then presented.

3.1. Deformation and failure behaviour

For 20Y–CSZ, fracture is brittle at 23° C (Fig. 1); crystal orientation is indicated by the stereographic triangle. However, as the test temperature rises, the

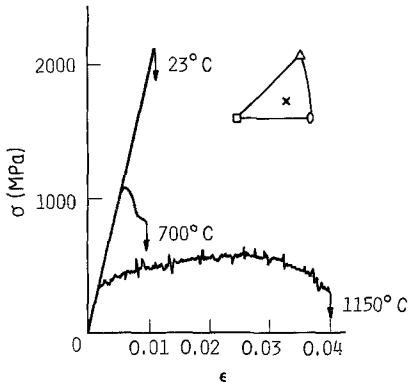

Figure 1 Compressive stress against strain for 20Y–CSZ single crystal.

*Ceres Corporation, Waltham, Massachusetts, USA.
†Nilsen TS-Grade PSZ; Nilsen Sintered Products Ltd, Northcote, Victoria, Australia.

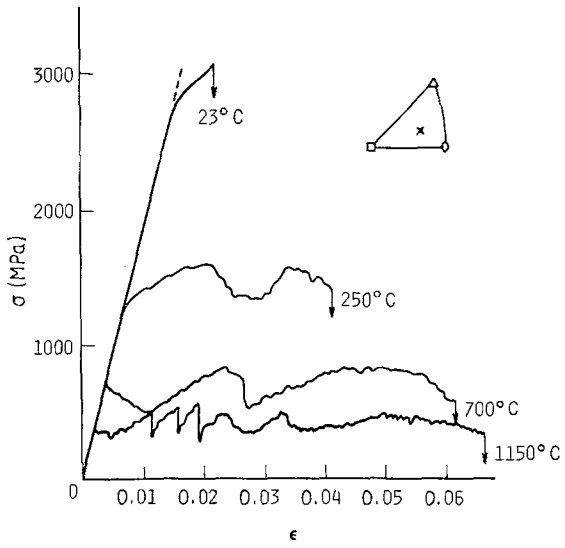

Figure 2 Compressive stress against strain for 5Y–PSZ crystal.

material yields and flows, with the plastic strain at failure approaching 4% at 1150° C. At the latter temperature the crystal hardens very little, and plastic flow is "jerky".

On the other hand, 5Y–PSZ (Fig. 2) fails following plastic flow at 23° C, and at this temperature it is considerably stronger than cubic material under equivalent conditions. The strength of the partially stabilized ceramic decreases quite rapidly with increasing temperature, while the extent of plastic flow concurrently increases, reaching nearly 7% at 1150° C. For temperatures $\gtrsim 250°$ C, flow is again rather jerky.

By way of comparison, the strength of polycrystalline Mg–PSZ (Fig. 3) is essentially independent of temperature to 1000° C [11]. Like the single crystals, however, this material also exhibits plastic behaviour; this flow is serrated, the amplitude of the local load drops increasing with temperature.

It is interesting that the single crystals emit no acoustic emission (AE) prior to yielding. In a few cases, AE was detected after several per cent of plastic strain, although the most common observation was little or no AE until failure. Similarly, the polycrystalline material exhibited AE for stresses above yielding, but below ultimate, only for temperatures $< 500°$ C, above which only the failure event itself yielded detectable stress waves [11]. These results suggest that significant flow takes place prior to the nucleation of

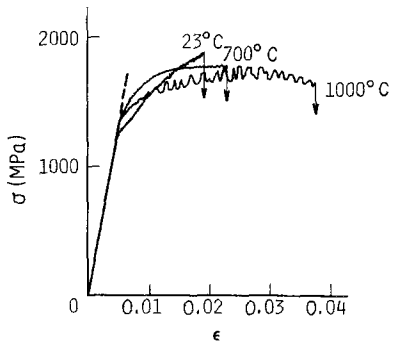

Figure 3 Compressive stress against strain for polycrystalline Mg–PSZ.

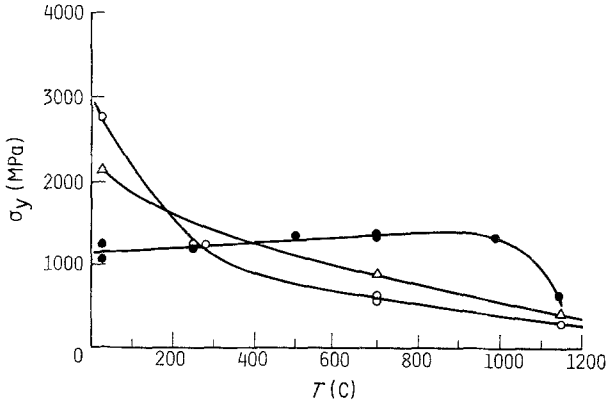

Figure 4 Yield strength against temperature for all three ceramics. (△) 20Y–PSZ, (○) 5Y–PSZ, (●) Mg–PSZ.

microcracks; subsequent microscopy will show that this is indeed the case.

The temperature dependence of yield strength (σ_y) is summarized for all three materials in Fig. 4. Here the continuously decreasing plastic flow resistance of both fully and partially stabilized zirconia contrasts with the essentially constant-strength polycrystalline material. Ultimate compressive (σ_c) strengths follow the same qualitative trends (Fig. 5), while flexural strengths (σ_t) decrease only slightly with increasing temperature. Particularly noteworthy is the fact that while $\sigma_c/\sigma_t \simeq 4$ for polycrystalline Mg–PSZ from 23 to 1200° C, the same ratio for 20Y–CSZ and 5Y–PSZ drops from ~ 8 and ~ 3, respectively, at 23° C, to ~ 1 at $T \simeq 1000°$ C. The value of σ_c/σ_t for brittle materials is usually about 8; it will be recalled that within the present series of tests, only 20Y–CSZ at 23° C exhibited brittle failure.

Fig. 6 shows strain to failure for all three materials over the temperature range 23 to 1200° C. It is clear that despite similarities in $\sigma_y(T)$ and $\sigma_c(T)$, plastic deformation in 5Y–PSZ differs both in its extent and, possibly, its mechanism, from that of 20Y–CSZ. As discussed in the next section, the latter seems to be true.

3.2. Deformation and fracture mechanisms

It was shown elsewhere [11] that polycrystalline Mg–PSZ fails by the nucleation, during plastic flow, of a myriad of tiny, grain-sized, axial microcracks, which eventually combine to cause failure. Their

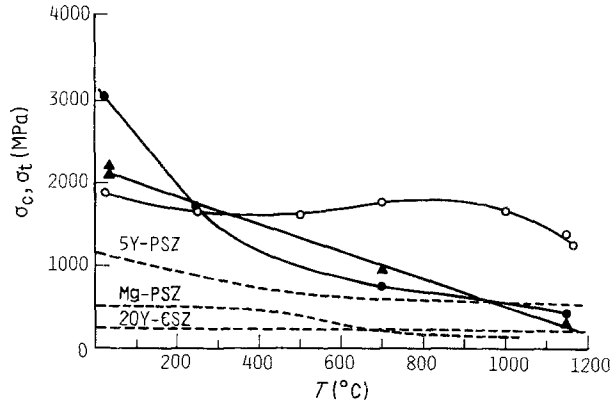

Figure 5 Compressive and flexural strength against temperature for all three ceramics. (▲) 5Y–PSZ, (○) Mg–PSZ; (—) σ_c, (– – –) σ_t.

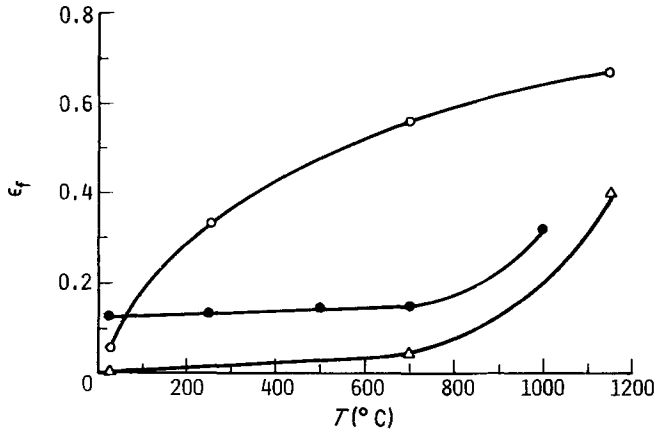

Figure 6 Strain at failure against temperature for all three ceramics. (△) 20Y–CSZ, (○) 5Y–PSZ, (●) Mg–PSZ.

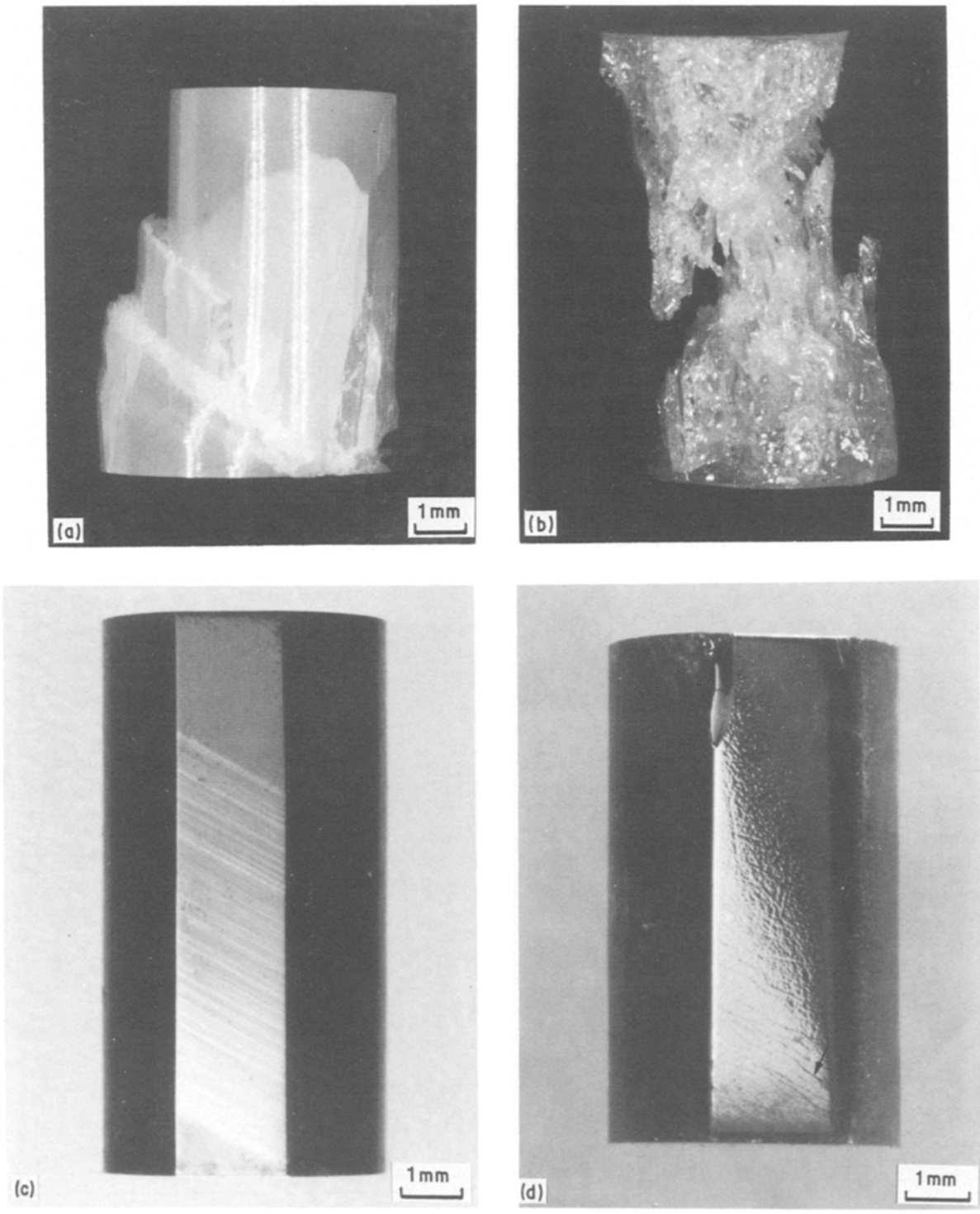

Figure 7 Macroscopic views of fracture and deformation. (a) Shear fracture, 5Y–PSZ, 700° C; (b) fracture by coalescence of multiple shear microcracks, 20Y–PSZ, 700° C; (c) planar slip bands, 5Y–PSZ, 700° C, ε_p = 1.5%; (d) apparent wavy slip bands (arrow), 20Y–CSZ, 700° C, ε_p = 1.5%.

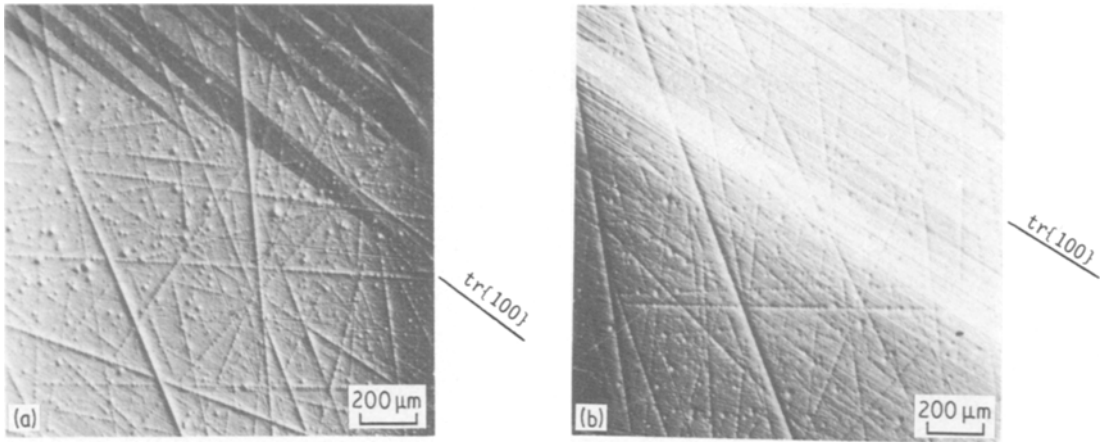

Figure 8 High-magnification Nomarski photos of 5Y–PSZ specimen shown in Fig. 7(c), T = 700C, ε_p = 1.5%. Slip bands and twins superimposed on polishing marks. (a) Upper end, macroscropic twins; (b) upper end of planar slip bands.

sudden coalescence usually causes the specimen to essentially explode. The single crystals studied here behaved in a decidedly different fashion; for purposes of example, photomicrographs of specimens tested at 700° C are used, results at other temperatures differing chiefly in degree.

Specimens compressed to failure, i.e. a state of negligible load-bearing capacity, are shown in Figs 7a and b. The 5Y–PSZ crystal fails by sliding on several distinct, macroscopic shear planes, while the 20Y–CSZ specimen has failed due to the coalescence of multiple shear microcracks, following extensive plastic flow within the shear bands. It should be noted that the latter specimen is still intact. Part of the path each of these specimens followed to failure is shown in Figs 7c and d, which represent specimens compressed to 1.5% plastic strain (ε_p).

At this juncture the 5Y–PSZ crystal has slipped on planar slip bands over some three-quarters of its length, with the bands having progressed from the lower end of the specimen. Not readily visible in the photo are macroscopic twins near the upper end, which share the same crystallographic trace as the slip bands. The 20Y–CSZ specimen, on the other hand, has developed what might best be described as wavy deformation bands (arrow), and no twins. Also visible in the Nomarski illumination are what appear to be an array of surface dimples. Axial microcracks are not present on either specimen.

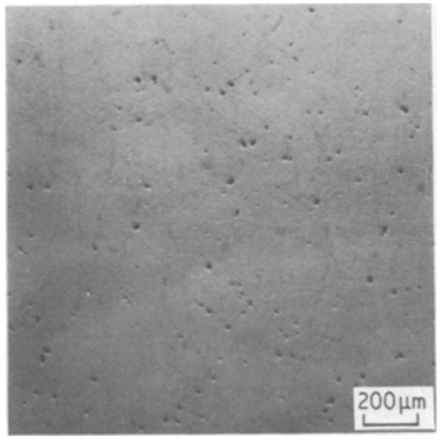

Figure 9 Polished flat, Nomarski illumination, 5Y–PSZ, prior to test (no deformation).

Higher magnification views of these specimens reveal interesting details. For example, the twins in the upper portion of Fig. 7c, shown in Fig. 8a, apparently extend almost all the way across the specimen. Furthermore, they are superimposed upon what appear to be rather coarse polishing marks – scratches which appear far too coarse to correspond to a 0.05 μm finish. The planar slip bands shown in Fig. 8b lie in an identical field of scratches. Since the polishing marks outside the slip band field are sharper than those within it, it would appear that the formation of the scratches preceded the slip bands.

This is not as trivial a statement as it might seem, because the "polishing marks" were invisible prior to the test. Fig. 9 shows a Nomarski view of a polished flat on an untested 5Y–PSZ specimen. Evidently, compressive stress caused the polishing marks to become visible, and apparently prior to extensive plastic deformation.

Laue X-ray diffraction was used to establish the crystallography of the twins and the slip bands. It was determined thereby that the planar slip system was $\{0\,0\,1\}\langle 0\,1\,1\rangle$, and that the trace of the twin planes was $\{0\,0\,1\}$.

Deformation details of the cubic zirconia were strikingly different. As shown in Fig. 10a, intense wavy slip bands seemed to lie predominantly along $\{1\,1\,1\}$; however, these were connected by diffuse secondary slip bands with an unusual "feathery" appearance, as shown in Fig. 10b. Polishing scratches are again visible, but only major ones, and these seem to be made up of rows of dimples. Looking again at Fig. 8, it can be seen that these polishing marks are likewise formed of dots, but they are much smaller and closer together than for the cubic material.

The preceding observations suggest that some sort of transformation must occur within both CSZ and PSZ due to the imposition of compressive stresses. Transmission electron microscopy of 5Y–PSZ surface replicas shadowed at very low angles indicates that transformations also occur during polishing (Fig. 11). Here the optically smooth surface can be seen to be covered, over about 50% of its area, with small,

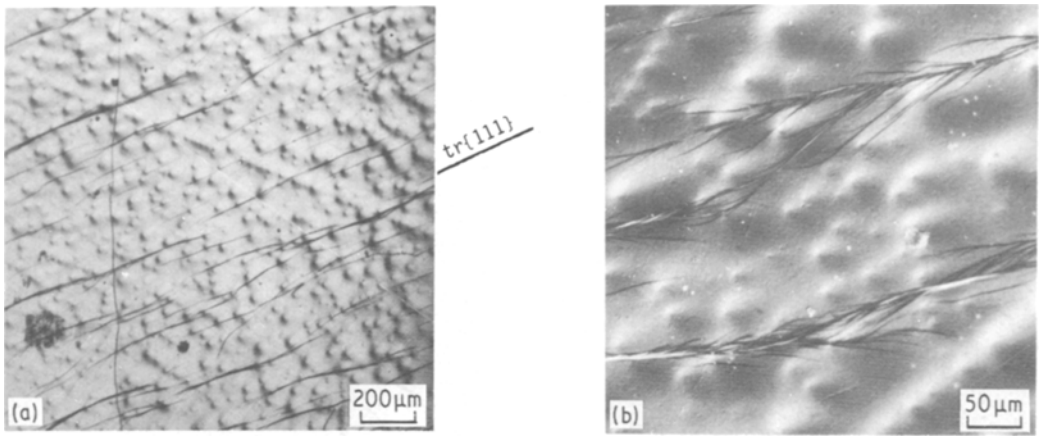

Figure 10 High magnification Nomarski photos of 20Y–CSZ specimen shown in Fig. 7d, $T = 700°$ C, $\varepsilon_p = 1.5\%$. Slip bands superimposed on polishing marks and dimples. (a) Wavy slip bands connected by "feathery" slip; polishing marks formed by rows of dimples; (b) high-magnification view of "feathery" slip.

rumpled, apparently transformed domains. Close inspection indicates that some of these may be internally twinned.

Compressive deformation causes further transformation, as shown in Fig. 12a. In this case, it appears that the transformed particle density is not as great as in Fig. 11, suggesting that the polishing-induced transformation may revert under the action of compressive stress. Close observation of polishing marks shows that they are actually composed of clusters of transformed microdomains – the "dots" seen in Figs 8 and 10. Study at high magnification (Fig. 12b) shows that the slip bands are composed of numerous closely-spaced slip lines, and that the transformed particles have a distinct internal structure.

Raman spectroscopy was used to evaluate the phases present on the 5Y–PSZ flat shown in Fig. 8. Careful study showed absolutely no monoclinic phase, indicating that the transformations which reveal the scratches are not of the type tetragonal → monoclinic.

Transmission electron microscopy of both undeformed [4] 5Y–PSZ specimens and ones deformed in compression at 283° C (Fig. 13a), shows a "tweed" structure composed of cubic and tetragonal domains. Dislocations (arrows) are visible in the deformed structure; further TEM work is in progress to establish whether they lie within the active $\{1\,0\,0\}\langle 1\,1\,0\rangle$ slip system.

At 700° C, and a plastic strain of ~ 1.5% (compared with the preceding ~0.5%), the microstructure is highly distorted, as shown in Figs 13b and c. The original "tweed" structure is very difficult to recognize, and domains appear faulted; by changing the diffraction conditions, what appear to be extended partial dislocations (arrows, Fig. 13c) can be discerned lying on certain faults.

Interestingly, preliminary TEM study of polycrystalline Mg–PSZ compressed to a strain of ~0.5% at 23° C shows no evidence of dislocation activity. However, the lattice is highly strained by tetragonal to monoclinic transformations, so that any dislocations would be very difficult to distinguish.

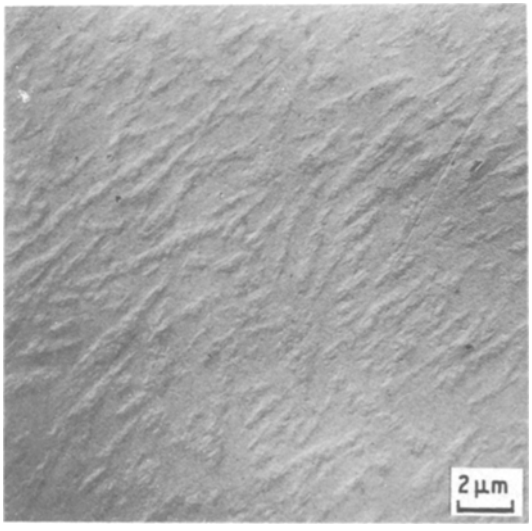

Figure 11 TEM replica, 5Y–PSZ, undeformed; surface rumpling due to transformations induced by polishing (same surface as that in Fig. 9).

4. Discussion

The preceding results are surprising and interesting in a number of ways, with regard to both mechanical behaviour and microstructural development. Furthermore, they may have implications with regard to other factors such as fracture toughness.

The extreme temperature sensitivity of σ_y and σ_c for both 5Y–PSZ and 20Y–CSZ is at variance with the equivalent tensile strengths. This is probably due to the fundamentally different processes involved in tensile and compressive failure. During a tensile test, the stress field may cause very limited plastic flow, as observed by Ingel *et al.* [1, 2], but before this becomes a factor, i.e. before plastic instability can set in, the specimen inevitably fails by nucleating a single fatal crack at some intrinsic flaw. Since the latter process is not affected by a slight amount of general plastic flow, σ_T is relatively independent of temperature.

During compression, however, microcracks do not form until considerable plastic strain has accumulated. Since no grain boundaries are available to block slip lines, flow takes place in continuous bands across the specimen; shear cracks eventually form within the

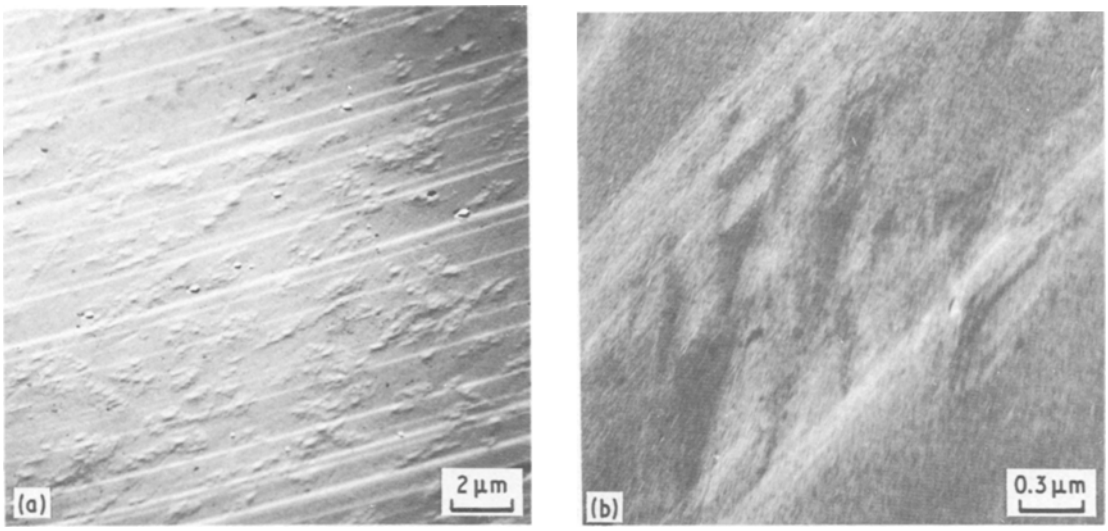

Figure 12 TEM replica, 5Y–PSZ, 700° C, $\varepsilon_p = 1.5\%$. (a) Overall view, slip bands and surface rumpling caused by transformations; (b) slip band microstructure, shape and internal structure of transformed microdomains.

slip bands, and the specimens lose their load-bearing capacity (i.e. they fail). This process is facilitated in 5Y–PSZ by the semicoherent nature of the tetragonal precipitates and their cubic parent phase. As the tetragonal c/a ratio is nearly unity, the slip process is basically occurring in a cubic system, which permits planar slip. As the temperature rises, slip becomes easier, and plastic instability (Figs 7a and b) sets in at progressively lower stress.

The fact that $\sigma_c \simeq \sigma_T$ for $T \gtrsim 900°$ C is probably coincidental, since failure is achieved by entirely different mechanisms. This contrasts with the case for polycrystalline ceramics [11–13], in which failure in both tension and compression involves subcritical tensile microcracks. The latter are simply harder to nucleate and propagate in compression, so that σ_c/σ_T is consistently $\gtrsim 4$ for such materials.

In an earlier paper [14], it was concluded that the serrated "flow" of polycrystalline Mg–PSZ was caused by co-operative shear of tetragonal particles producing bands of transformed monoclinic material. Since this process is not very sensitive to temperature, and since failure occurs by the usual mechanism of nucleation and coalescence of axial microcracks, $\sigma_c/\sigma_T \gg 1$ over a wide range in temperature. However, for the single-crystal materials the flow-stress

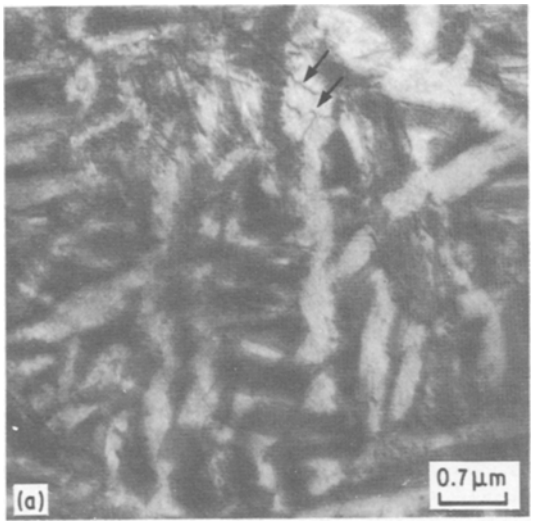

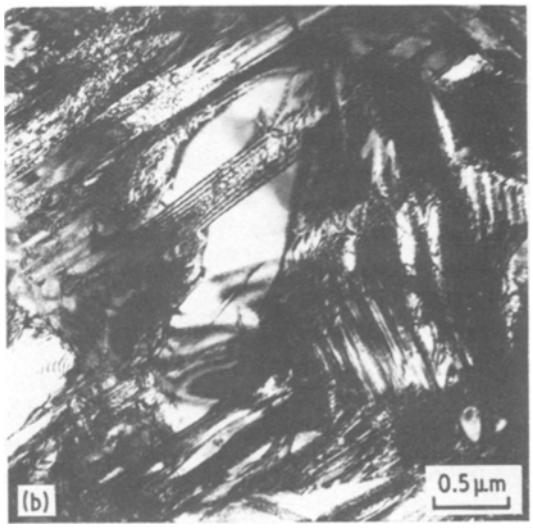

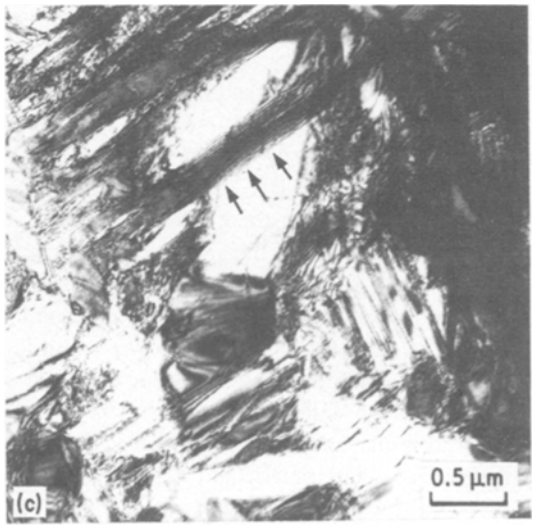

Figure 13 Transmission electron microscopy of deformed 5Y–PSZ. Foils are normal to stress axis. (a) $T = 283°$ C, $\varepsilon_p \simeq 0.5\%$; tweed microstructure, arrows indicate dislocations; (b) $T = 700°$ C, $\varepsilon_p \simeq 1.5\%$; distorted and faulted microstructure; (c) altered contrast, same region as in (b), showing possible extended dislocations (arrows) in fault.

load drops probably have a different origin, namely the sequential activation of individual planar (5Y–PSZ) and wavy (20Y–CSZ) slip bands. In this case the serrations are extremely relevant, as they represent events which are directly responsible for the development of the plastic instability which leads to failure.

With this point in mind, it is obvious that crystallographic orientation probably was important in the failure of the single crystals. The chosen orientation amounted to provision of the possibility of easy glide on essentially any low-index slip system. For the 5Y–PSZ material, it would be interesting to explore the effect of testing crystals in orientations for which $\{0\,0\,1\}\langle 0\,1\,1\rangle$ is hard to operate, the hardest being $\{0\,0\,1\}$ aligned with the compression axis. If the activation of a secondary system such as $\{1\,1\,1\}\langle 1\,1\,0\rangle$ were sufficiently difficult, the crystals would be forced to fail in a brittle fashion, i.e. by nucleating axial microcracks. The compressive strength would then be much less sensitive to temperature, and should more or less maintain its ambient strength as the test temperature is increased.

For the cubic 20Y material, such a plan is less likely to succeed, since it is impossible to orient a cubic crystal in such a way that every $\{1\,1\,1\}\langle 1\,1\,0\rangle$ system is totally inaccessible. However, a near $\langle 1\,1\,1\rangle$ axis would be fairly hard for this slip system.

The $\{0\,0\,1\}\langle 0\,1\,1\rangle$ slip observed for 5Y–PSZ crystals is in agreement with the earlier work by McCartney *et al.* [8] on Ca–CSZ crystals compressed along the same axis at 1350° C. What is surprising is the seemingly unusual $\{1\,1\,1\}$ wavy slip experienced by 20Y–CSZ. However, it was noted by Hannink and Swain [6] that for yttria-stabilized cubic zirconia, hardness anisotropy was compatible with *either* $\{0\,0\,1\}\langle 0\,1\,1\rangle$ or $\{1\,1\,1\}\langle 1\,1\,0\rangle$. That being the case, it is possible that for 20Y–CSZ, $\{1\,1\,1\}\langle 1\,1\,0\rangle$ slip dominates for $T \lesssim 700°$ C, while the $\{0\,0\,1\}\langle 1\,1\,0\rangle$ system is active at higher temperatures. In addition, it will be recalled that Michel *et al.* [3] observed cleavage on $\{1\,1\,1\}$ for 16.2Y–CSZ crystals failed in bending, while Ingel [4] observed that the crystallographic dependence of K_{Ic} for 20Y–CSZ exhibited a minimum along $\{1\,1\,1\}$. Actually, the waviness and "feathery" slip prevalent in 20Y–CSZ (Fig. 10) suggests that multiple slip systems are involved for $T \lesssim 700°$ C.

Recalling Fig. 5, it appears that $\sigma_c(T)$ for 5Y–PSZ may be composed of two branches with different slopes, the transition between these occurring around $300° \text{ C} < T < 500°$ C. It is possible that the lower-temperature branch corresponds to $\{1\,1\,1\}\langle 1\,1\,0\rangle$ slip, while the high-temperature regime relates to flow on $\{0\,0\,1\}\langle 0\,1\,1\rangle$. Further TEM and X-ray slip trace analysis is in progress to test these possibilities.

The principal implication of the surface transformation observations is that they are not caused by tetragonal → monoclinic; rather, they probably are due to reversible [9] transformation (rhombohedral → cubic) of rhombohedral domains produced by polishing the cubic (20Y–CSZ) or cubic–tetragonal (5Y–PSZ) starting material. Since polishing marks were revealed during compression tests performed at temperatures as low as 250° C, it is not likely that the transformations were thermal in origin. Raman spectroscopy showed no evidence of monoclinic phase on transformed surfaces, and Nomarski study of regions around diamond pyramid indentations in both CSZ and PSZ crystals showed absolutely no evidence of the characteristic co-operative shear bands created in such tests by tetragonal → monoclinic transformations [15].

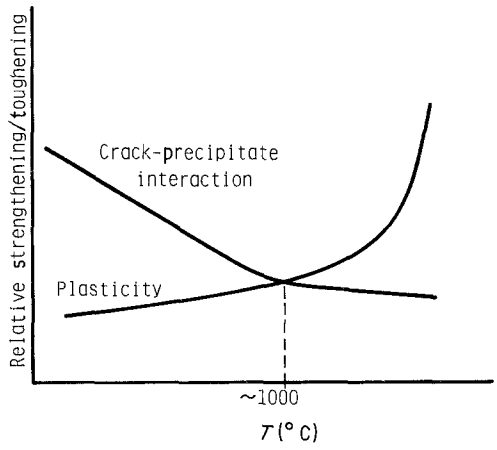

Figure 14 Conceptual model of temperature dependence of strengthening/toughening in Y–PSZ single crystal.

These findings are in basic agreement with those of Hasegawa [9], regarding the production of rhombohedral (r) material by the polishing of yttria-stabilized zirconia containing, or composed of, cubic phase. In his study, less r-phase was produced by polishing high-Y (more cubic) material, which correlates with the present observation that only very intense polishing scratches in 20Y–CSZ seemed to transform under compression.

Based on these observations, it would appear that the strength and toughness of 5Y–PSZ and 20Y–CSZ single crystals have little or nothing to do with phase transformations. The tetragonal → monoclinic transformation does not occur either in tension [3, 5] or compression, and the stress-assisted rhombohedral transformation is probably superficial and not capable of controlling bulk properties. The complex $K_c(T)$ behaviour observed by Ingel *et al.* [2] must require an explanation based on crystallographic orientation, microcleavage along certain planes, temperature-dependent plastic flow, and crack–precipitate interaction.

A simple view of such a concept is shown in Fig. 14. At lower temperatures, crack-growth resistance would be governed largely by crack–precipitate interactions, which result from lattice, elastic and thermal expansion mismatches between the cubic matrix and its tetragonal precipitates. As the temperature rises, these contributions will decrease, probably faster than the increase in plasticity contribution, which will be orientation-dependent as well. At elevated temperatures, plasticity will dominate, producing an apparent high toughness.

5. Conclusions

1. Compressive yield and ultimate strengths for 5Y–PSZ and 20Y–CSZ single crystals decrease rapidly with increasing temperature.

2. Plastic flow in 5Y–PSZ is planar on $\{1\,0\,0\}$, while slip in 20Y–CSZ is wavy on $\{1\,1\,1\}$ and secondary systems.

3. Tetragonal → monoclinic transformations do not occur during compressive loading in either single-crystal variant.

4. Compressive stresses appear to reverse cubic → rhombohedral transformations induced by polishing in both 5Y–PSZ and 20Y–CSZ.

Acknowledgements

The support of the Office of Naval Research under Contract No. N00014–84–C–0213 is gratefully acknowledged. Thanks are expressed to R. W. Rice for provision of the single crystals, and to T. W. Coyle who performed Raman spectroscopy of a deformed specimen.

References

1. R. P. INGEL, R. W. RICE and D. LEWIS, *J. Amer. Ceram. Soc.* **65** (1982) C108.
2. R. P. INGEL, D. LEWIS, B. A. BENDER and R. W. RICE, *ibid.* **65** (1982) C-150.
3. D. MICHEL, L. MAZEROLLES and M. PEREZ y JORBA, *J. Mater. Sci.* **18** (1983) 2618.
4. R. P. INGEL, PhD dissertation, Catholic University of America (1982).
5. T. W. COYLE, PhD dissertation, Massachusetts Institute of Technology (1985).
6. R. H. J. HANNINK and M. V. SWAIN, unpublished work (1985).
7. C. A. BROOKES, J. B. O'NEIL and B. A. W. REDFERN, *Proc. R. Soc.* **A332** (1971) 73.
8. M. L. McCARTNEY, W. T. DONLON and A. H. HEUER, *J. Mater. Sci.* **15** (1980) 1063.
9. H. HASEGAWA, *J. Mater. Sci. Lett.* **2** (1983) 91.
10. T. SAKUMA, Y.-I. HOSHIZAWA and H. SUTO, *ibid.* **4** (1985) 29.
11. J. LANKFORD, *J. Mater. Sci.* **20** (1985) 53.
12. *Idem, J. Amer. Ceram. Soc.* **64** (1981) C33.
13. *Idem*, in "Fracture Mechanics of Ceramics", Vol. 5, edited by R. C. Bradt, A. G. Evans, D. P. H. Hasselman and F. F. Lange (Plenum Press, New York, 1983) p. 625.
14. *Idem, J. Amer. Ceram. Soc.* **66** (1983) C212.
15. R. H. J. HANNINK and M. V. SWAIN, *J. Mater. Sci.* **16** (1981) 1428.

Received 4 July
and accepted 8 August 1985